https://doi.org/10.15407/ujpe65.3.247

B.V. BILANYCH,[1] O. SHYLENKO,[2] V.M. LATYSHEV,[2] A. FEHER,[2] V.S. BILANYCH,[1]
V.M. RIZAK,[1] V. KOMANICKY[2]

[1] Faculty of Physics, Uzhhorod National University
(Uzhhorod 88000, Ukraine)
[2] Faculty of Science, Safarik University
(Kosice 04001, Slovakia)

INTERACTION OF CHALCOGENIDE $\mathbf{As_4Se_{96}}$ FILMS WITH ELECTRON BEAM WHEN USED AS ELECTRONIC RESISTS

The interaction of an electron beam with chalcogenide films As_4Se_{96} has been studied. The kinetics of the formation of an electron-induced surface relief in the dose range 9.3×10^3–9.3×10^7 $\mu C \cdot cm^{-2}$ is established. The parameters of the interaction of a film As_4Se_{96} with an electron beam are calculated. It is shown that the observed point of inversion of the shape of the electron-induced relief can be caused by the crossover of the surface potential. The process of manufacturing the image element by the single-step lithography is realized on the surface of an As_4Se_{96} film.

Keywords: chalcogenide glass, thin films, As–Se, electron-induced surface relief.

1. Introduction

Chalcogenide films exhibit the sensitivity to light irradiation which has been exploited in the production of functional devices for microelectronics, integrated optics, and holograms. The mechanism of photoinduced processes involves the photogeneration and the interaction of charges, which lead to various structural changes. The intense generation of charges within a chalcogenide film occurs also under the electron irradiation. Investigations of the interaction of electron beams with chalcogenide films of the binary compositions As-Se [1], Ge–Se [2], and Sb–Se [3] have shown the formation of surface reliefs of various types depending on the charge deposited in a film. The recent studies of ternary chalcogenide systems based on Ge–As–Se have revealed unique electron-induced effects such as the electro-hydrodynamic instability [4] or inversion of the shape of an electron-induced surface relief [5, 6].

The binary As–Se systems have a very high sensitivity to the irradiation. As shown in Ref. [7], a change in the direction of the lateral mass transport can be observed in the As_xSe_{100-x} films with $x = 4.5$ during the formation of a photoinduced surface relief. The change occurs specifically in the low As concentration range (critical concentration $x = 4$ at.% As) and is caused by a topological transition of the As_xSe_{100-x} glass structure from a one-dimensional annular structure to a one-dimensional chain one. When $2 < x < 6$ at.% As, the zero hole mobility is observed [8].

Electron beam-induced phenomena are related to the charge dissipation which can involve the charge transport by both electrons and holes. Taking the above-mentioned facts into account, we have chosen the As_4Se_{96} system. This system exhibits also the extremely high sensitivity to the action of an electron beam, so we studied a possibility of using this

---

material for the high-speed fabrication of protective elements by the one-stage (dry) lithography. In this work, we will carefully determine the interaction with an electron beam in the range of radiation doses from 3×10^3 to 9.3×10^7 μC $\cdot$ cm^{-2}.

2. Experimental Details

For this study, the amorphous films of As_4Se_{96} with a thickness of 4 μm were prepared. These films were obtained by the thermal evaporation in vacuum using a glass of the same chemical composition. The films were deposited on sapphire substrates at a rate of 10 nm/s. Freshly prepared films were used in the measurements.

The films were irradiated with electrons using a scanning electron microscope (SEM) Tescan, model VEGA. The following parameters were used: the accelerating voltage $V = 30$ kV, spot size $B = 0.64$ μm, and electron beam current $I = 60$ nA. The irradiation dose was determined by the formula $G = I \times t/S$, where S is the cross-section area of an electron beam focused on the film surface; t is the time of irradiation. The exposure times were changed from 0.05 ms to 5 s, the time dependence of the exposure dose was calculated by the formula $G = 18.6 \times 10^6 \times t$, ($\mu$C $\cdot$ cm^{-2}). To facilitate the surface charge removal, the irradiation of the films was carried out in a low-vacuum atmosphere of nitrogen at a residual pressure of 10 Pa. The structure of the induced surface reliefs on the film surface was studied using an atomic force microscope (AFM) (Bruker, ICON model) in the "tapping mode".

3. Results of Experiments

The irradiation of films was carried out during the exposure times from 0.05 ms to 5 s, which determined doses in the range from 9.3×10^2 to 9.3×10^7 μC $\cdot$ cm^{-2}. For each individual dose G, a square matrix (20×20) of point-irradiated regions was made on the surface of the film. The matrix period d was 10 μm. The value of d was chosen large enough to avoid the proximity effects [9]. To study the surface relief in the irradiated regions, the surface was scanned by AFM. Figure 1 shows the AFM scans of the irradiated regions of As_4Se_{96} films and the profiles of the electron beam-induced surface reliefs. From Fig. 2, it can be seen that the kinetics of surface relief formation for As_4Se_{96} films in the range from 9.3×10^2 to 9.3×10^7 μC $\cdot$ cm^{-2} is characterized by three ranges of radiation doses in which reliefs of different shapes are formed

- Below $G < 1.2$ μC $\cdot$ cm^{-2} ($t < 65$ μs), the cones with a Gaussian profile are formed;
- 1.2 μC $\cdot$ cm^{-2} $< G <$ 46.5 μC $\cdot$ cm^{-2} (65 μs $< t <$ 2.5 ms) – the dose range in which the height h_1 of formed cones of the Gaussian type remains practically unchanged;
- 46.5 μC $\cdot$ cm^{-2} $< G <$ 9.3×10^4 μC $\cdot$ cm^{-2} (2.5 ms $< t <$ 5 s) is the range of doses in which craters of the same type are formed with depth h_2.

Ranges 2 and 3 are separated by the inversion point [10] – the irradiation dose G_i at which the shape of the surface relief changes – from a cone to a crater.

In Fig. 2, the dependences of the surface relief parameters h, S, and d on the irradiation time are given, where: h is the height (depth), S is the cross-section area, and d is the half-width of the surface cone (crater). It can be seen from Fig. 2 that these parameters of the surface relief of films depend on the irradiation time. When constructing their time dependences in the coordinates $\lg t$ on the graphs, rectilinear sections are observed.

In particular, an increase in h_1 occurs with increasing t in the interval 40–65 μs. The linear approximation of the dependence of $h(t)$ on the value $h = 0$ indicates that the maximum irradiation time (for the selected electron beam parameters) at which the surface relief did not appear is 32 μs ($G_0 \approx 600$ μC $\cdot$ cm^{-2}). In the interval 65±80 μs, the value of $h(t)$ remains almost unchanged. At $t > 80$ μs, the value of h_1 decreases, and, subsequently, the cone turns into a crater whose depth h_2 increases with t. With an increase in t in the interval 80 μs $< t <$ 5 s, the dependence $h(t)$ can be approximated by a decreasing straight line in the coordinates "h-$\lg t$". The intersection of this line with the abscissa axis gives the inversion point at $t = 2.5$ ms (inverse dose $G_0 = 46.5 \times 10^3$ μC $\cdot$ cm^{-2}).

The changes in S and d during the irradiation on a logarithmic scale have a linear dependence in individual intervals. In particular, in the interval 0.04 ms $< t <$ 1 ms, the cross-section area of the cones increases linearly. Further, as the irradiation time increases to the inversion point, S decreases. Later on, at the irradiation, craters with increasing parameters h_2 and S are formed.

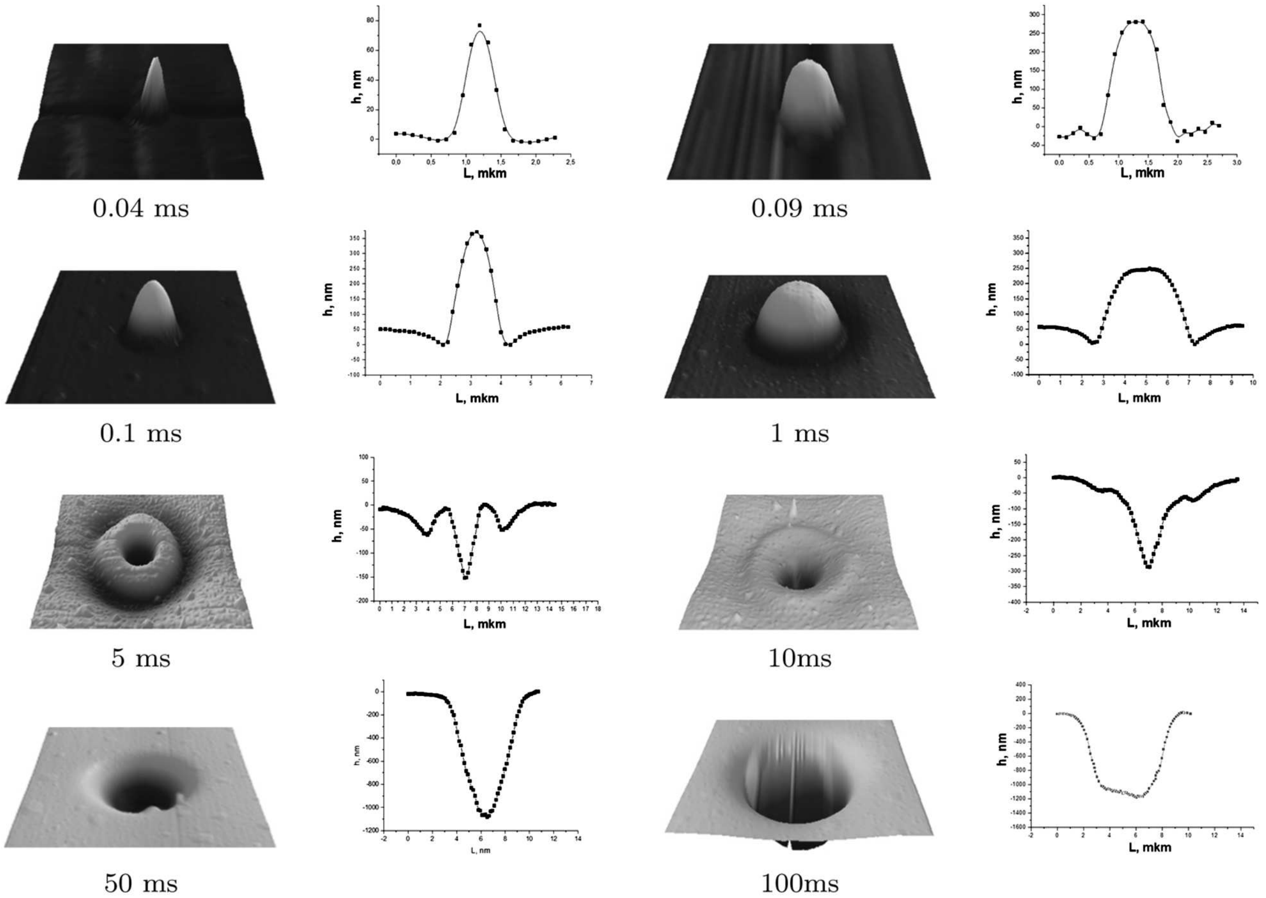

0.04 ms 0.09 ms

0.1 ms 1 ms

5 ms 10ms

50 ms 100ms

Fig. 1. AFM images and surface relief profiles induced by an electron beam on the surface of the As_4Se_{96} film which are formed at different irradiation times

The diameter of the relief of the irradiated region d in the "d-lg t" coordinates increases linearly in the interval 0.04 ms $< t < 50$ ms. Subsequently, with increasing t, the parameter d is not changed.

4. Discussion

The kinetics of formation of a surface relief and changes in its shape and parameters during the electron irradiation of the As_4Se_{96} film can be explained using the charge model which was used earlier for Ge–As–Se films [6]. The mechanism of formation of various types of a surface relief in this model is the electrostatic interaction in the space charge region caused by the formation of two dynamically changing charged layers which are induced in the chalcogenide film during its electron irradiation.

It is known that when the electron beam hits the film surface, various physical phenomena related to the transmission of the energy of electrons to the exposed material in the irradiated region occur. The transfer of the energy of electrons occurs during their inelastic collision with atoms of the film being studied in the region of their interaction. The R value of the interaction region for the As_4Se_{96} film was calculated by the Kanaya–Okayama formula [11]:

$$R = 0.0276\,\frac{A\,E_0^{\frac{5}{3}}}{\rho\,Z^{\frac{8}{9}}}, \qquad (1)$$

where A is the average atomic weight, Z is the average charge of the nucleus, ρ is the density of the irradiated substance, E_0 is the energy of primary electrons.

When calculating the parameter R for the As_4Se_{96} film, the following numerical values were taken: $A = 78.84$ (g/mol), $Z = 33.96$, $\rho = 4.33$ g/cm^3, $E_0 = 30$ keV. The average atomic weight A and the av-

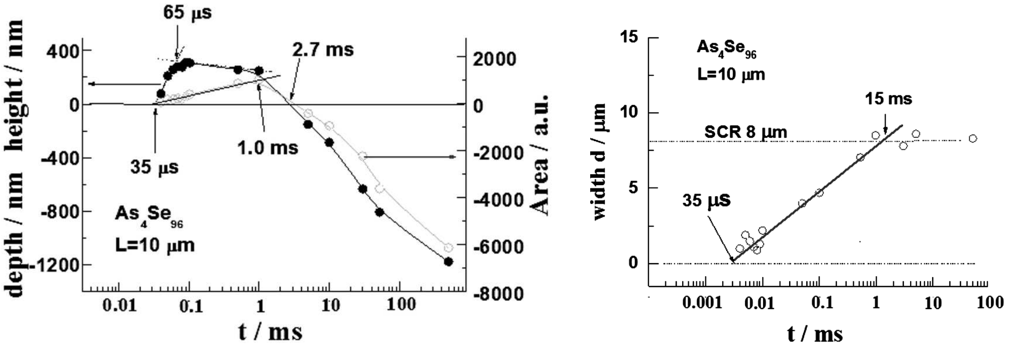

a *b*

Fig. 2. Changes of the parameters of the electron-induced surface relief of an As_4Se_{96} film depending on the irradiation time: height – the height of the cones, depth – the depth of the craters, area – the axial section area, d – the half-width

erage nuclear charge Z were determined by the formulas: $A = c_1A_1 + c_2A_2$ and $Z = c_1Z_1 + c_2Z_2$, where $c_1 = 0.04$, $c_2 = 0.96$, – As and Se concentrations, and A_1, A_2, and Z_1, Z_2 are their atomic weights and nuclear charges, respectively. As a result of this calculation, the value $R \approx 6.3$ μm was obtained.

The shape of the interaction region depends on the average nucleus charge Z of atoms of the substance, electron energy, and angle of incidence of a beam. In our case, the shape of the interaction region is close to a spherical surface with a transverse dimension of 6.3 μm [12]. In this region, under the electron irradiation influence, a space charge region is formed and causes the formation of a surface relief in the chalcogenide film.

The mechanism of charging the film involves the competition between the number of incident electrons which penetrate into the film and generate charges along their movement trajectory and the numbers of ejected secondary and backscattered electrons from the sample to vacuum.

When the electron irradiation penetrates the As_4Se_{96} film, electrons and holes are generated by primary electrons. The scattered energy of incident electrons partially goes to the formation of non-equilibrium electron-hole pairs, causing a substantial increase in the number of mobile charge carriers. The average energy of formation of an electron-hole pair for As_4Se_{96} ($2 \approx$ eV [13]) is much smaller than the energy of the incident electron. Therefore, one electron with an energy of 30 keV along its trajectory in a chalcogenide film can create several thousand electron-hole pairs.

As a result of the penetration of primary electrons into the film and their capture at deep and shallow energy levels, a negative charge Q_- is formed in the film. Its thickness is equal to the penetration depth of incident electrons into the sample. Due to the emission of secondary electrons from the near-surface layers of the film back into vacuum, a relatively thin near-surface layer with positive charge Q_+ is formed. In other words, at the electronic irradiation, the charge accumulates in the volume and on the film surface. These two layers of charges (Q_- and Q_+) create an electric field in the region of interaction of the film and the electron beam [14]. As a consequence, a potential V_s appears on the film surface, and its magnitude and sign depend on the total charge $\Delta Q = |Q_- - Q_+|$ [15]:

$$V_s = \frac{\Delta Q h}{\varepsilon_0 \varepsilon_r S} + \frac{(Q_+ l + Q_- R)}{2\varepsilon_0 \varepsilon_r S}, \qquad (2)$$

where S is the area of the irradiated region, h is the film thickness, ε_0 and ε_r are the dielectric constant of vacuum and the material, respectively.

The appearance and magnitude of the charges Q_+ and Q_- determine the shape and parameters of the surface relief of the film as a result of its expansion or contraction during the electrostatic interaction in the irradiated region.

It is known that a positive charge is formed in non-conducting materials in the near-surface region under the electron irradiation [16]. It can be assumed that the formation of a charge Q_+ in the near-surface layer of the As_4Se_{96} film at the irradiation leads to the film expansion (due to the electrostatic repulsion). The height of the surface relief in the form of a cone increases with the irradiation time up to 65 μs (Fig. 2). Taking the electron emission coefficient σ into account, the accumulated positive charge can be determined by the formula $Q_+ = \sigma I_0 t_+ = (\eta + \delta) I_0 t_+$, where σ is the electron emission coefficient, $I_0 = 60$ nA is the electron beam current, δ and η are the coefficients of secondary and backscattered electrons, respectively, t_+ is the rise time of a surface relief of the film (cone) at the initial stage of irradiation ($t_+ = 65$ μs). The reflection coefficient η of the investigated chalcogenide film can be calculated from the formula [17]:

$$\eta(Z, E_0) = C E_0^m, \tag{3}$$

where $m(Z) = 0.1382 - \frac{0.9211}{\sqrt{Z}}$, $C(Z) = 0.1904 - 0.2235 \ln Z + 0.1292 (\ln Z)^2 - 0.01491 (\ln Z)^3$, where Z is the average charge of an atomic nucleus. As a result, the following values were obtained: η (As_4Se_{96}) ≈ 0.29, (for sapphire, η (Al_2O_3) $= 0.037$). The coefficient of secondary emission δ does not depend monotonically on Z [18]. For the As_4Se_{96} film, Z is 33.96 and, according to [18], we took $\delta \approx 0.3$ and $Q_+ = 2.3$ pC, subsequently. The use of a low-pressure nitrogen in a SEM chamber also supplements the formation of a positive charge on the film surface.

The average depth of the yield of secondary electrons for the As_4Se_{96} film was calculated by the formula [19]:

$$\lambda = \frac{0.267 A_0 I}{\rho Z^{\frac{2}{3}}} \text{ [nm]}, \tag{4}$$

where A_0 is the atomic weight, Z is the ordinal number, ρ is the matter density, and I is the first ionization potential (9.56 eV for As_4Se_{96} [20]). The depth of the yield of secondary electrons for the As_4Se_{96} film is $\lambda = 4.4$ nm. The depth of the output of reflected electrons X_η is determined by the empirical formula [21]:

$$x_\eta = R\, 0.45\, \mathrm{e}^{-0.22(Z+1)}. \tag{5}$$

For the As_4Se_{96} film with $x_\eta = 1.3$ μm,a layer of negative charge appears in the film due to the inelastic scattering of primary electrons in the interaction region, and their capture by deep centers and various defects. The total negative charge $Q_- = (1 - \eta) I_0 t$, which is formed in the film depth, is determined by the total irradiation time. It also depends on changes in η during the irradiation due to the presence of a surface (positive or negative) potential Vs. The changes of $\eta(t)$ for the As_4Se_{96} film are not known. For $\eta(t) = \text{const} = 0.41$, $t = 0.5$ with $Q_- = 12.3$ nC.

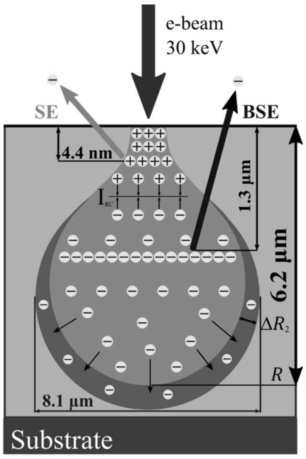

Fig. 3. Schematic diagram of the space charge region formed during the interaction of a primary electron beam with As_4Se_{96}. (SE – secondary electrons, BSE – backscattered electrons). Primary electron beam can shift or change the energy (decelerate), when the surface potential becomes negative

It is seen from Fig. 2 that the area of the axial section of the surface cones S increases linearly to $t = 1$ ms. It can be assumed that, at $t = 1$ ms, the positive charge maximally spreads over the surface in the irradiation region. The increase in $d(t)$ at $t > 1$ ms indicates a further increase in the charge accumulated region. At $t > 50$ ms, $d(t) \approx \text{const} = 8.1$ μm. This value is comparable to the value of the interaction region $R \approx 6.3$ μm for the As_4Se_{96} film. We can assume that, with the chosen parameters of the electron irradiation, the time of the formation of a SCR in this film is 50 ms. A higher value of $d > R$ in this case may be due to the partial diffusion of charges from the interaction region into the depth of the film by an amount ΔR. Proceeding from the obtained numerical values of the parameters of the interaction of the film with the electron beam, it is possible to represent the charge model for the As_4Se_{96} film (Fig. 3) [6].

4.1. Electronic lithography on As_4Se_{96} film

The appearance of a surface relief of various shapes on an As_4Se_{96} film under the electron irradiation indicates a possibility of using this material as an elec-

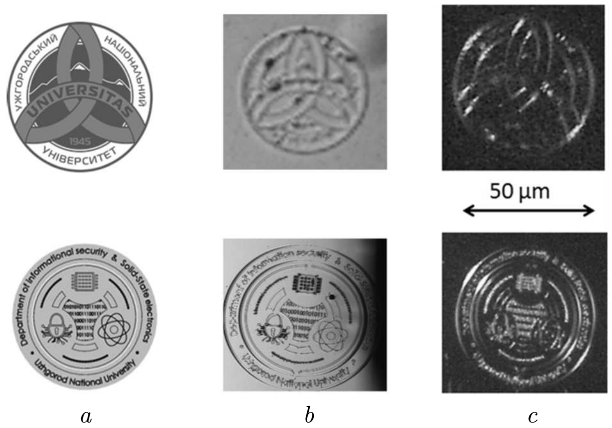

Fig. 4. View of the university and department logoses (*a*), their images on the surface of As_4Se_{96} film in the optical mode of an atomic-force microscope (*b*), and the images of the logoses after their metallization (*c*)

tronic resist for a single-stage (without chemical etching) electron lithography. The characteristic points (irradiation doses) and the parameters of the interaction of the electron beam with the As_4Se_{96} film calculated above make it possible to implement a negative (film expansion and the formation of cones) or positive (film compression and the crater formation) lithography on this film.

Using the DrawBeam software module included in the SEM software, the standard images were taken by the negative (Fig. 4, *a*) and positive (Fig. 4, *b*) electron lithography methods on the As_4Se_{96} film. In addition, the images of some logoses on this film were made, which can be used to create the master-originals of protective elements. The images of the logoses are shown in Fig. 4. Figure 4, *d* shows the images of these logoses produced on the surface of the film. The local irradiation dose in the lithographic process causing to the maximum height of the surface relief (Fig. 2) was 1.2 $\mu\mathrm{C}\cdot\mathrm{cm}^{-2}$, which corresponds to an irradiation time of 65 μs. As a result, the height of the surface relief that forms the image data was about 270 nm. The obtained metallized (Ti) surface images are shown in Fig. 4, *c*.

As can be seen from Fig, 4, despite the rather large diameter of the electron beam (640 nm), all the image elements are clearly visible. Therefore, it can be assumed that making the large-sized surface images (>1 mm) will significantly improve their quality. Moreover, using the thinner (≈5 nm) electron beams will make it possible to obtain high-quality images in the nano-area.

5. Conclusions

Three intervals of radiation doses of the As_4Se_{96} film in which the processes of charge accumulation and redistribution occur in the region of its interaction with the electron beam are determined. The threshold (G_0) and inverse (G_i) radiation doses, as well as the parameters of the charge model for the investigated film, are determined. The possibility of using this film for the single-stage electron lithography is shown. Images of some logoses that can be used to make protective holograms are made on the surface of the As_4Se_{96} film.

This work has been supported the grant of the Slovak Research and Development Agency under the contract No. APVV-17-0059. The author Bogdan Bilanych is grateful to a grant of National Scholarship Programme of the Slovak Republic SAIA for the financial help in the realization of this research.

1. K. Tanaka. Electron beam induced reliefs in chalcogenide glasses. *J. Appl. Phys.* **70**, 261 (1997).
2. Galen B. Hoffman, Ronald M. Reano. Electron beam direct write of chalcogenide glass integrated optics. *J. Vacuum Sci. Technol.* **30**, 06F301 (2012).
3. O. Shiman, V. Gerbreders, A. Gulbis. The interaction between electron beam and amorphous chalcogenide films. *J. Non-Cryst. Sol.* **358**, 1876 (2012).
4. V. Bilanych, V. Komanicky, M. Lackova *et. al.* Fabrication of meso- and nano-scale structures on surfaces of chalcogenide semiconductors by surface hydrodynamic interference patterning. *Mater. Res. Express* **2**, 105201.1 (2015).
5. V. Kuzma, V. Bilanych, M. Kozejova *et. al.* Study of dependence of electron beam induced surface relief formation on Ge–As–Se thin films on the film elemental composition. *J. Non-Crystal. Sol.* **456**, 7 (2017).
6. V. Bilanych, V. Komanicky, M. Kozejova *et. al.* Surface patterning of Ge–As–Se thin films by electric charge accumulation. *Thin Solid Films* **616**, 86 (2016).
7. M.L. Trunov, P.M. Lytvyn. Selective light-induced mass transport in amorphous As_xSe_{100-x} films driven by the composition tuning: Effect of temperature on maximum acceleration. *J. Non-Crystal. Sol.* **493**, 86 (2018).
8. V.I. Mikla. Distinct topological regimes in binary As_xSe_{100-x} glasses. *J. Phys.: Condens. Matter* **9**, 9209 (1997).
9. T.H.P. Chang. Proximity effect in electron-beam lithography. *J. Vac. Sci. Technol.* **12**, 1271 (1975).
10. V. Bilanych, V. Komanicky, A. Feher *et. al.* Electron-beam induced surface relief shape inversion in amorphous $Ge_4As_4Se_{92}$ thin films. *Thin Solid Films* **571**, 175 (2014).

11. K. Kanaya, S. Okayama. Penetration and energy-loss theory of electrons in solid targets. *J. Phys. D* **5**, 43 (1972).
12. R. Shimizu, T. Ikuta, T.E. Everhart *et. al.* Experimental and theoretical study of energy dissipation profiles of keV electrons in polymethylmethacrylate. *J. Appl. Phys.* **46**, 41581 (1975).
13. L. Tichy, H. Ticha, P. Nagels *et. al.* Optical properties of amorphous As-Se and Ge–As–Se thin films. *Mater. Lett.* **39**, 122 (1999).
14. E.N. Evstaf'eva, E.I. Rau, V.N. Mileev *et. al.* Analysis of mechanisms of dielectric target charging under the effect of electron irradiation. *Inorg. Mater.: Appl. Res.* **2**, 106 (2011).
15. A.V. Gostev, E.N. Evstaf'eva, E.I. Rau *et. al.* Characteristics of dielectric film charging, depending on their thickness upon electron irradiation. *Bulletin Russ. Acad. Sci. Phys.* **78**, 833 (2014).
16. M. Bai, R.F.W. Pease, C. Tanasa *et. al.* Charging and discharging of electron beam resist films. *J. Vac. Sci. Technol.* 17, **6**, 2893 (1999).
17. H.J. Hunger, L. Kuchler. Measurements of the electron backscattering coefficient for quantitative EPMA in the energy range of 4 to 40 keV. *Phys. Stat. Sol.* **56**, K45 (1979).
18. K. Ohya, T. Ishitani. Target material dependence of secondary electron images induced by focused ion beams. *Surf. Coat. Technol.* **158**, 8 (2002).
19. S. Ono, K. Kanaya. The energy dependence of secondary emission based on the range-energy retardation power formula. *J. Phys. D: Appl. Phys.* **12**, 619 (1979).
20. Ch.E. Moore. *Ionization Potentials and Ionization Limits Derived from the Analysis of Optical Spectra* (NSRDS-NBS 34, 1970).
21. E.I. Rau, S.A. Ditsman, S.V. Zaitsev *et. al.* Analysis of formulas for calculating the main characteristics of backscattered electrons and how they compare to experimental results. *Bulletin of the Russ. Acad. Sci. Phys.* **77**, 951 (2013).

Received 21.09.19

Б.В. Біланич, О. Шиленко,
В.М. Латишев, A. Feher, В.С. Біланич,
В.М. Ризак, V. Komanicky

ВЗАЄМОДІЯ ХАЛЬКОГЕНІДНИХ ПЛІВОК As_4Se_{96} З ЕЛЕКТРОННИМ ПУЧКОМ ПРИ ВИКОРИСТАННІ ЇХ У РОЛІ ЕЛЕКТРОННИХ РЕЗИСТІВ

Резюме

Досліджено взаємодію електронного пучка з халькогенідними плівками As_4Se_{96}. Встановлена кінетика формування електронно-індукованого рельєфу поверхні в дозовому діапазоні $9{,}3 \cdot 10^3$–$9{,}3 \cdot 10^7$ мкС $\cdot$ см$^{-2}$. Розраховано параметри взаємодії плівки As_4Se_{96} з електронним пучком. Показано, що спостережувана точка інверсії форми електронно-індукованого рельєфу може бути зумовлена кроссовером поверхневого потенціалу. На поверхні плівки As_4Se_{96} був реалізований процес виготовлення елемента зображення методом одноступеневої електронної літографії.